Biomolecules & Biomedicine

Biomolecules and Biomedicine
ISSN: 2831-0896 (Print) | ISSN: 2831-090X (Online)

Journal Impact Factor® (2022): 3.4
CiteScore® (2022): 5.3
www.biomolbiomed.com | blog.biomolbiomed.com

RESEARCH ARTICLE

ALKBH5 promotes hepatocellular carcinoma cell proliferation, migration and invasion by regulating *TTI1* expression

Qimeng Chang[1,2*], Xiang Zhou[1,2*], Huarong Mao[1,2], Jinfeng Feng[1,2], Xubo Wu[1,2], Ziping Zhang[1,2#], Zhiqiu Hu[1,2#]

[1]Department of Hepatobiliary-Pancreatic Surgery, Minhang Hospital, Fudan University, Shanghai, China

[2]Institute of Fudan-Minhang Academic Health System, Minhang Hospital, Fudan University, Shanghai, China

#Corresponding authors: Zhiqiu Hu; Email: huzq@fudan.edu.cn; Ziping Zhang; Email: zhang_zp@fudan.edu.cn

Associate editor: Dengming He

[*]**These authors contributed equally.**

DOI: https://doi.org/10.17305/bb.2024.10247

Submitted: 07 January 2024/ **Accepted:** 07 March 2024/ **Published online:** 18 March 2024

Conflicts of interest: Authors declare no conflicts of interest.

Funding: This work is supported by Medical Research Specialized Program of Beijing Huatong Guokang Foundation for Industry-University-Research Innovation Fund of Chinese Universities, National Ministry of Education (2023HT060 to ZQH).

Data availability: The datasets used and/or analyzed during the current study are available from the corresponding author on reasonable request.

ABSTRACT

The objective of this research was to investigate the potential mechanisms of AlkB homolog 5, RNA demethylase (*ALKBH5*) in hepatocellular carcinoma (HCC). We used The Cancer Genome Atlas (TCGA), Kruskal-Wallis method and Kaplan-Meier (KM) survival analysis to study the expression of *ALKBH5* and its correlation with clinical factors in HCC. *In vitro* experiments verified the expression of *ALKBH5* and its effect on HCC cell phenotype. We screened differentially expressed genes (DEGs) from HCC patients associated with *ALKBH5*. Through this screening we identified the downstream gene *TTI1* which is associated with *ALKBH5* and investigated its function using gene expression profiling interaction analysis (GEPIA) along with univariate Cox proportional hazards regression analysis. Finally, we analyzed the functions of *ALKBH5* and *TTI1* in HCC cells. Across numerous pan-cancer types, we observed significant overexpression of *ALKBH5*. *In vitro* experiments confirmed *ALKBH5* as an oncogene in HCC, with its knockdown leading to suppressed cell proliferation, migration, and invasion. Bioinformatics analyses also demonstrated a significant positive correlation between *ALKBH5* and *TTI1*. *TTI1*, highly expressed in cells, showed promising prognostic ability for patients. Further experiments confirmed that suppressing *TTI1* impeded cell growth and movement, with this effect partially offset by increased *ALKBH5* expression. Conversely, promoting these cellular processes was observed with *TTI1* overexpression, but was dampened by decreased *ALKBH5* expression. In conclusion, our findings suggest that *ALKBH5* may influence proliferation, migration and invasion of HCC by modulating *TTI1* expression, providing a new direction for treating HCC.

KEYWORDS: Liver hepatocellular carcinoma, *ALKBH5*, *TTI1*, proliferation, migration, invasion

INTRODUCTION

Liver carcinoma, characterized as a malignant neoplasm, has been extensively linked with risk factors such as excessive alcohol consumption, viral hepatitis, consumption of mold-contaminated food, and genetic predispositions (1). This disease can be histopathologically subdivided into two principal categories: Hepatocellular carcinoma (HCC) and intrahepatic cholangiocarcinoma (iCCA)(2). HCC, accounting for 90% of primary liver cancer cases, represents the predominant histological subtype of this malignancy. Key contributory factors implicated in HCC include aflatoxin exposure, obesity, epigenetic alterations, heredity, infection with the hepatitis C virus, tobacco smoking, chronic hepatitis B, and diabetes (3). Currently, among methods for HCC treatment, transplantation is the most effective (4). Interventional therapy, ablation therapy, chemoradiotherapy, and targeted therapy can be applied to patients with unresectable liver carcinoma (5, 6). Regrettably, despite these interventions, the prognosis for HCC remains dismal due to high rates of metastasis and recurrence (7). This highlights the necessity of uncovering the molecular processes driving HCC progression and pinpointing new therapeutic targets.

The AlkB homolog 5, RNA demethylase (*ALKBH5*), also known as ABH5, OFOXD, or OFOXD1, is implicated in the biological cascades of various neoplasms (8). Notably, Guo et al. showed that *ALKBH5* could curb pancreatic carcinoma progression through PER1 activation in an m6A-YTHDF2-mediated pathway. This finding reveals that *ALKBH5* inhibits pancreatic cancer by regulating the post-transcriptional activation of PER1 through modulation of m6A modifications(9). And there have been previous studies describing the role of *ALKBH5* in liver

cancer. For example, *ALKBH5* may be a key effector associated with macrophage M2 polarization. the *ALKBH5*/SOX4 axis promotes hepatocellular carcinoma stem cell properties through activation of the SHH signaling pathway(10). Circ-CCT3 is subjected to *ALKBH5*- and METTL3-mediated m6A modification and promotes hepatocellular carcinoma development through the miR-378a-3p-FLT1 axis(11). *ALKBH5* acts as a dual role of a microenvironmental regulator and a radiosensitization target, mediating monocyte recruitment and M2 polarization and creating positive feedback to reduce HCC radiosensitivity(12). *ALKBH5*-mediated lincRNA affects HCC growth and metastasis requiring methylation(13).*ALKBH5* promotes HCC growth, metastasis and macrophage recruitment through the *ALKBH5*/MAP3K8 axis(14). It had been reported not only in cancer, but also in disease such as another literature by Chen et al. established that *ALKBH5* selectively augments the incidence of acute myeloid leukemia (AML) and the self-renewal of carcinoma stem cells(15). Moreover, *ALKBH5* has been reported to function as a tumor promoter in AML by post-transcriptionally modulating pivotal targets, such as TACC3(16) , an oncogene related to prognosis in a broad spectrum of carcinomas(17-20). Together, these observations underscore the central function of *ALKBH5* in the pathogenesis of leukemia and the self-renewal of leukemia stem cells/leukemia-initiating cells (LSC/LIC), thereby highlighting the role of *ALKBH5*/N6-methyladenine (m6A) axis for therapeutic potential. These revelations pave the way for further exploration of the roles played by *ALKBH5* in the pathogenesis of diverse human carcinomas.

Our research attempted to illuminate the role of *ALKBH5* in HCC, utilizing an integrative

91 approach of bioinformatics analysis and cellular experiments. In parallel, we worked to
92 uncover the precise mechanism by which *ALKBH5* and HCC are interconnected. It is
93 anticipated that our findings may provide new insights and pave the way for advances in
94 therapeutic intervention, diagnosis, and prognostic assessment of HCC patients.
95

96 **MATERIALS AND METHODS**

97 **Evaluation of *ALKBH5* expression levels across pan-cancers**

98 To assess the expression levels of *ALKBH5* across a range of cancer types, we utilized data
99 procured from The Cancer Genome Atlas (TCGA; https://tcga-data.nci.nih.gov/tcga) and the
100 Genotype-Tissue Expression (GTEx; https://www.gtexportal.org/home/) database. The TCGA
101 includes large multidimensional map of key genomic changes in various cancers. On the other
102 hand, the GTEx project provides a valuable resource that facilitates the study of human gene
103 expression and regulation in different tissue types. By integrating these resources, we
104 conducted a pan-cancer study exploring *ALKBH5* expression across 33 cancer types, in
105 comparison to normal tissues. The analysis was executed using R software, offering a
106 comprehensive visual depiction of *ALKBH5* expression distribution.
107

108 **Correlation analysis between *ALKBH5* expression and HCC clinical parameters**

109 HCC samples were obtained from the TCGA for comprehensive surveys. We used the Kruskal-
110 Wallis method to analyze the differential expression of *ALKBH5* in the context of multiple
111 clinical parameters of HCC, including nodal status (node), metastatic status (metatasis), pT
112 stage, pTNM stage, grade, HBV and HCV. This nonparametric statistical test allowed us to
113 compare expression levels across numerous independent groups. Subsequently, to graphically

114 illustrate the mutual relationships and transitions among these clinical parameters, *ALKBH5*
115 expression, and patient status, we employed the "ggplot2" package in R to generate an
116 informative and visual Sankey diagram. This diagram serves to provide an intuitive
117 understanding of the interplay among these key aspects.
118
119 **Analysis of functional pathways in differentially expressed genes (DEGs)**
120 According to the expression of *ALKBH5* in HCC, we divided the TCGA-HCC patient data into
121 *ALKBH5*-high and *ALKBH5*-low cohorts for screening DEGs. Subsequently, we screened for
122 up-regulated DEGs ($P<0.05$ and fold change (FC) >1.5) and down-regulated DEGs ($P<0.05$
123 and FC <0.67) using the Limma package in R software. Next, to further elucidate the biological
124 roles of the DEGs, we performed Kyoto Encyclopedia of Genes and Genomes (KEGG)
125 pathway enrichment analysis using the Enrichr tool (https://maayanlab.cloud/Enrichr/).
126 Findings with a *P*-value below 0.05 were deemed to be of statistical relevance.
127
128 **Analysis of genes associated with prognosis of HCC**
129 We performed a progression-free survival (PFS) analysis of 100 up-regulated and 100 down-
130 regulated DEGs. Statistical tests for differences in PFS between low and high expression
131 groups were performed using the log-rank test in Kaplan-Meier (KM) survival analysis, and
132 hazard ratios (HR), 95% confidence intervals (CI), and *P* values were subsequently generated.
133 From this survival analysis, we focused on genes with *P* values less than 0.05, indicating
134 statistical significance. To gain a comprehensive understanding of the protein-protein
135 interaction (PPI) associated with these genes, we exploited the potential of the proteins encoded

by statistically significant genes. We used the Search Tool for the Retrieval of Interacting Genes (STRING) STRING database (https://string-db.org/) as the primary platform for interactive data. Additionally, network visualization and analysis were performed using Cytoscape software. Subsequently, for the genes that showed statistical significance in the survival analysis, we performed a gene correlation analysis, the results of which were visualized by the R package "heatmap".

Screening of candidate genes in the prognostic model

We utilized Least Absolute Shrinkage and Selection Operator (LASSO) regression, implemented through the "glmnet" package in R, to construct a polygenic signature for prognostic prediction of HCC using genes that displayed significant *P* values. To ensure the reliability and objectivity of the analysis, ten-fold cross-validation was conducted to select the optimal lambda (λ) value that corresponds to the smallest error fraction. Subsequently, HCC patients were divided into high-risk and low-risk groups, and their survival time, risk score, as well as survival status were obtained from the selected dataset. The z-scores of 6 gene expression (*TTI1*, *ACIN1*, *ADNP*, *CFHR3*, *SPP2*, *HGFAC*) in these patients were displayed by heat map. Ultimately, the prognostic implications of the high-risk and low-risk groups were substantiated through KM survival analysis. To identify significant variations in PFS probability between the two groups, a log-rank test was carried out. Additionally, time-dependent receiver operating characteristic (ROC) analysis for 1-year, 3-year, and 5-year survival forecasts was used to assess the prognostic performance of the risk model. The area under the curve (AUC) method was used to determine the prediction accuracy of the model.

Correlation analysis between *ALKBH5* and candidate target genes

As a newly developed interactive web server, Gene Expression Profiling Interactive Analysis (GEPIA) offers features that are customized, which are inclusive of patient survival analysis and gene detection. In this study, we employed GEPIA to investigate the relationship between *ALKBH5* and potential target genes. Through the computation of correlation coefficients, we identified a key gene displaying the strongest correlation with *ALKBH5* and HCC. When the $P<0.05$, the results were deemed statistically significant.

Construction and verification of the predictive nomogram with TTI1

Initially, we evaluated the expression level of TTI1 in HCC samples utilizing the Wilcoxon test. Subsequently, the prognostic significance of TTI1 was compared with clinical parameters, such as pM stage, pT stage, pTNM stage, age, and grade, through a univariate Cox proportional hazards regression analysis. In order to ascertain if TTI1 could function as an independent prognostic factor for risk stratification in HCC patients, a multivariate Cox proportional hazards regression analysis was executed. This analysis incorporated additional clinical parameters that exhibited statistical significance ($P<0.05$) in the univariate Cox regression model. Based on the independent prognostic factors identified from the preceding analyses, a composite nomogram was constructed via the "rms" package in R. This predictive tool was designed to forecast 1-year, 3-year, and 5-year survival probabilities, and its performance was subsequently assessed through a calibration curve.

Cell culture and transfection

We procured LO2 (normal liver cell), MHCC-97L, MHCC-97H and SNU387 (HCC cell lines) from American Type Culture Collection (ATCC, Manassas, USA). LO2 cells were maintained in IMDM-RMPI supplemented with 1% penicillin-streptomycin and 10% fetal bovine serum (FBS), while MHCC-97L, MHCC-97H, and SNU387 cells were cultured in DMEM, fortified with the same supplements. All cell lines were incubated at 37°C in an environment containing 5% CO_2. For cell transfection, we acquired si-ALKBH5 #1, si-ALKBH5 #2, si-ALKBH5 #3, over-ALKBH5, si-TTI1 #1, si-TTI1 #2, si-TTI1 #3, over-TTI1, along with their negative controls (over-NC and si-NC) from the Shanghai Biotech Company, Gemma Gene. Transfection was carried out using Lipofectamine 3000 (Invitrogen), and the efficiency of this process was evaluated under a fluorescence microscope.

RNA extraction and quantitative real-time polymerase chain reaction (qRT-PCR) analysis

TRIzol (Invitrogen) was used to extract the total RNA from the cells. The RevertAid First Strand cDNA Synthesis Kit from Invitrogen was used to create complementary DNA (cDNA). qRT-PCR was carried out using an Applied Biosystems 7900 Real-time PCR System and the SYBR Green PCR Master Mix. The $2^{-\Delta\Delta Ct}$ technique was used to compare the relative expression levels of *ALKBH5* and *TTI1*, with *GAPDH* acting as an internal control. The following primers were used in this experiment: *ALKBH5* (forward: 5'-CGGCGAAGGCTACACTTACG-3'; reverse: 5'-CCACCAGCTTTTGGATCACCA-3'), TTI1 (forward: 5'-CCACAGCTGAAGACATCGAA-3'; reverse: 5 '-

202 ACATCTGGACGGGTGTCATT-3') and GAPDH (forward: 5'-
203 CAAGGTCATCCATGACAACTTTG -3'; reverse: 5'- GGGCCATCCACAGTCTTCT -3').
204
205 **Western Blotting (WB) assay**
206 ALKBH5 and TTI1 protein expression in HCC cell lines were evaluated using a WB assay.
207 Cells underwent lysis and protein extraction with RIPA buffer containing a protease inhibitor
208 cocktail. Protein concentrations were determined via a BCA assay kit. Proteins were then
209 subjected to SDS-PAGE and transferred to PVDF membranes. Post-transfer, membranes were
210 blocked using 5% non-fat milk for non-specific binding prevention. They were then probed
211 overnight at 4°C with primary antibodies for ALKBH5 (1:1000) and TTI1 (1:500). GAPDH
212 (1:1000) served as the control. After washing, membranes were exposed to HRP-linked
213 secondary antibodies (1:5000) for an hour. Protein bands were detected with an enhanced
214 chemiluminescence (ECL) system and quantified by densitometry.
215
216 **Assay for cell proliferation**
217 CCK-8 kit (Shiga Doto Molecular Technology, Japan) was applied to measure cell proliferation.
218 First, we plated 2×10^4 of the transfected SNU387 cells in a 96-well plate in triplicate. Then,
219 10ul of CCK-8 solution per well was added into cells for the indicated time. After 24h, 48h,
220 72h, 96h, and 120h, we finished measuring the optical density (OD) value of the cells at 450
221 nm via iMark Microplate Reader (Bio-Rad) for plotting the cell proliferation curve.
222
223

Transwell assay

The invasive and migratory abilities of cells were determined utilizing a Transwell chamber assay (Corning). The upper chamber was covered with 100 l of Matrigel (Corning) and allowed to set up for an hour at 37 °C in preparation for the invasion assay. Subsequently, a 0.5μl cell suspension was added to the Matrigel-coated chamber, which was filled with DMEM medium devoid of serum. After the invasion and migration phases are complete, cells are stained with DAPI to reveal nuclei. High-resolution images were captured after a 20-minute staining period, utilizing an Olympus BX53 upright microscope equipped with a digital camera. The migration assay was performed in a similar manner, except the Matrigel coating step was omitted. Each of these experimental steps was independently replicated three times to ensure the accuracy and reproducibility of the findings.

Statistical analysis

R software was used for all statistical analyses. The Kruskal-Wallis or Wilcoxon test was used to analyze differences in expression among groups. The log-rank test was used to examine KM survival curves. Correlation coefficients were used to examine the relationship between ALKBH5 and clinical factors or prospective target genes. The prognostic model was built using LASSO regression with ten-fold cross-validation. To investigate prognostic value, univariate and multivariate Cox proportional hazards regression models were used. The *in vitro* experiments were conducted three times, and the results are reported as mean±standard deviation. Statistical significance was defined as $P<0.05$.

RESULTS

Significantly high expression of *ALKBH5* in the majority of pan-cancers

We have analyzed the expression levels of *ALKBH5* across 33 different human malignancies, utilizing data from both the TCGA and GTEx databases. As illustrated in Figure 1, *ALKBH5* exhibits significant overexpression in a majority of tumor tissues when compared to their neighboring normal tissues, including Breast invasive carcinoma (BRCA), adrenocortical carcinoma (ACC), cholangiocarcinoma (CHOL), and HCC, etc. This pattern of differential expression implies a potential role of *ALKBH5* in the oncogenesis and progression of these tumor types, warranting further investigation into its mechanistic contributions.

Effect of differential expression of *ALKBH5* in HCC on staging, HBV infection and patient survival

To elucidate the role of *ALKBH5* in HCC, we scrutinized its expression profile in relation to various clinicopathological parameters (Figures 2A-2G). Notably, *ALKBH5* expression showed significant variations between T2 and T3 stages, as well as between patients with and HBV+ and HBV- infection. In contrast, no substantial differences in *ALKBH5* expression were found when examined across other clinicopathological parameters. Furthermore, we observed a noteworthy interconnection between *ALKBH5* expression, clinical characteristics, and patient survival across different stages of HCC. A visual representation of these associations was provided in the form of a Sankey diagram (Figure 2H). The observed patterns suggest a potential differential role of *ALKBH5* in specific stages of tumor progression and in the context

268 of HBV infection. The association of *ALKBH5* expression with patient survival further implies
269 its potential as a prognostic marker in HCC.
270
271 **Knockdown of *ALKBH5* inhibits growth of HCC cells *in vitro***
272 We initially examined the expression of *ALKBH5* in HCC cell lines and normal cells. The
273 results demonstrated an upregulation of *ALKBH5* in HCC cell lines, particularly in the SNU387
274 and MHCC-97H cells, prompting us to select these cell lines for subsequent investigations
275 (Figure 3A). Next, we subjected the SNU387 and MHCC-97H cells to knockdown procedures,
276 finding that si-*ALKBH5* #1 demonstrated the highest efficiency and was consequently selected
277 for further experimentation (Figures 3B and 3C). Data from the CCK-8 assay revealed that the
278 knockdown of *ALKBH5* resulted in suppressed proliferation of SNU387 and MHCC-97H cells
279 (Figures 3D and 3E). Furthermore, results from the Transwell assay indicated that compared
280 with the si-NC transfected cells, SNU387 and MHCC-97H cells transfected with si-*ALKBH5*#1
281 exhibited significantly reduced invasion and migration capabilities (Figures 3F-3I). These
282 results suggest a critical function of *ALKBH5* in regulating the proliferative and metastatic
283 potential of HCC cells.
284
285 **KEGG pathway enrichment analysis on DEGs**
286 From the two groups of samples with differential expression of *ALKBH5*, we screened 3105
287 up-regulated DEGs and 156 down-regulated DEGs (Figure 4A). DEGs that were up-regulated
288 in the KEGG pathway were primarily enriched in Shigellosis, Focal adhesion, Regulation of
289 actin cytoskeleton, Proteoglycans in cancer, etc. (Figure 4B). DEGs that were down-regulated

290 in the KEGG pathway were primarily enriched in Retinol metabolism, Complement and
291 coagulation cascades, Chemical carcinogenesis-DNA adducts, etc. (Figure 4C).
292
293 **36 key genes associated with HCC prognosis**
294 In our analysis, we selected the top 100 up-regulated and 100 down-regulated DEGs for PFS
295 rate analysis. This led to the identification of 36 genes showing a significant association with
296 PFS (P<0.05) (Figure 5A). Interestingly, higher expression of genes such as *CHFR1*, *AZGP1*,
297 *APOC3*, and *ITIH1* was associated with a favorable prognosis, while the overexpression of
298 genes like *TBCCD1*, *ZNF362*, *ZNF318*, *ZMYM3*, *UBE3B*, and *TTI1* correlated with a poorer
299 prognosis. Further investigation into these 36 genes using the STRING database generated a
300 PPI network consisting of 36 nodes and 45 edges (Figure 5B). The correlation analysis revealed
301 significant positive or negative interactions among these 36 genes (Figure 5C). These findings
302 underscore the critical role of these genes in HCC progression and potentially highlight novel
303 prognostic markers for HCC.
304
305 **Identification of 6 candidate genes with prognostic value associated with HCC**
306 We utilized the glmnet package in R to construct a LASSO Cox regression model for the 36
307 genes with significant P values. With 10-fold cross-validation, we chose 0.0521 as the
308 minimum standard for λ (Figures 6A and 6B). Based on the non-zero coefficients of the genes,
309 we computed the risk score for each patient as follows:
310 (0.1124)*TTI1+(0.06)*ACIN1+(0.0402)*ADNP+(-0.0422)*CFHR3+(-0.0236)*SPP2+(-
311 0.0094)* HGFAC. We used the median cutoff point obtained from the "survminer" R package

312 to segregate the patients into high-risk (n=185) and low-risk (n=185) groups. As depicted in
313 Figure 6C, patients in the high-risk group demonstrated reduced survival time compared to the
314 low-risk group. The distribution of the six candidate prognostic genes also varied between the
315 two groups, with the expression of *ADNP*, *ACIN1*, and *TTI1* increasing as the risk score
316 escalated. Further, the KM survival curves indicated that the low-risk group had improved PFS
317 compared to the high-risk group (Figure 6D). Lastly, the risk model exhibited a substantial
318 AUC value of 0.704 in 1-year survival from the ROC analysis (Figure 6E). These findings
319 suggest that 6 candidate prognostic genes may be effective targets for predicting one-year
320 survival of HCC patients.
321

322 **Establishing *TTI1* as a key downstream gene of *ALKBH5***

323 We compared the association of six candidate genes with *ALKBH5* using the GEPIA database.
324 At a statistical significance threshold of $P<0.05$, a significant positive connection was observed
325 between *ALKBH5* and three genes (Figures 7A-7C). Among them, *TTI1* has the highest
326 correlation with *ALKBH5* (r=0.46), followed by *ADNP* (r=0.39) and *ACIN1* (r=0.36), therefore,
327 we identified *TTI1* as the key downstream gene of *ALKBH5*. *TTI1* expression was shown to be
328 considerably greater in HCC tumors than in normal tissues (Figure 7D). After *ALKBH5* was
329 overexpressed in SNU387 and MHCC-97H cells, qRT-PCR detected a significant
330 overexpression efficiency (Figure 7E). The results of CCK-8 showed that overexpressed
331 *ALKBH5* significantly promoted the proliferation of SNU387 and MHCC-97H cells (Figures
332 7F and 7G). Furthermore, we found that the expression of *TTI1* was decreased when *ALKBH5*
333 was knocked down, and conversely, the expression of *TTI1* was increased when *ALKBH5* was

overexpressed (Figures 7H and 7I). *TTI1* was discovered as an independent predictive predictor for overall survival (OS) in HCC patients in univariate and multivariate Cox proportional hazards regression studies (Figure 7J). In clinical practice, we developed a *TTI1* nomogram to estimate 1-, 3-, and 5-year survival in HCC patients (Figure 7K). The calibration plot indicated its predictions closely aligned with actual outcomes (Figure 7L).

ALKBH5 combined with _TTI1_ affects the proliferation, migration and invasion of HCC cells

Our study investigated the impact of *TTI1* knockdown in SNU387 and MHCC-97H cells. Through qRT-PCR, we found si-TTI1 #2 demonstrated the most significant knockdown efficiency (Figures 8A and 8B). To elucidate the functional mechanism of TTI1 and its upstream gene *ALKBH5* in HCC, we performed a CCK-8 assay. The results showed a decrease in cellular proliferation following the knockdown of *TTI1*. Interestingly, overexpression of *ALKBH5* could partially mitigate the suppressive effect of si-TTI1#2 on cell proliferation (Figures 8C and 8D). We also induced overexpression of *TTI1* in SNU387 and MHCC-97H cells (Figure 8E), which resulted in enhanced cellular proliferation, an effect which was diminished by the low expression of *ALKBH5* (Figures 8F and 8G). Further substantiating these observations, migration and invasion assays mirrored the trends witnessed in proliferation studies, indicating a tangible influence of *ALKBH5* and *TTI1* expression levels on the migratory and invasive potentials of HCC cells (Figures 8H-8O). Therefore, we posit that *ALKBH5*, through its regulatory action on *TTI1* expression, serves as a pivotal determinant in either promoting or inhibiting specific malignancy-associated cellular behaviors in HCC, underlining

356 a sophisticated network of genetic interactions pivotal to cancer cell dynamics.

357

358 **DISCUSSION**

359 We investigated the function of *ALKBH5* in the progression and prognosis of HCC in this study.
360 Consistent with the known risk factors for liver carcinoma, such as excessive alcohol
361 consumption, viral hepatitis, and genetic predispositions(21, 22), our findings further confirm
362 the complex and multifactorial nature of the etiology of HCC. Notably, we found an association
363 between high expression of *ALKBH5* and HCC. This adds a novel dimension to the already
364 complex landscape of HCC molecular mechanisms and provides fresh insights into potential
365 molecular targets for therapy. Our analysis underscored the prevalence of *ALKBH5*
366 overexpression in numerous tumor types, including HCC, thus augmenting its potential role as
367 a pan-cancer molecular marker. Furthermore, *ALKBH5* expression levels were consistently
368 greater in HCC clinical stage tissues compared to their normal counterparts, emphasizing its
369 likely significance in HCC pathological development. Intriguingly, we noted minimal variation
370 in *ALKBH5* expression across groups with differing clinical factors, suggesting that its
371 upregulation might be a universal event in HCC, independent of individual patient
372 characteristics. Our research serves as a seminal contribution towards comprehending the
373 molecular underpinnings of HCC and provides robust evidence implicating *ALKBH5* as a
374 potential therapeutic target.

375

376 The findings *in vitro* point to *ALKBH5* being a critical regulator of HCC cellular behavior,
377 influencing proliferation, migration, and invasion. We observed that ALKBH5 was

378 significantly overexpressed in HCC cell lines, especially in SNU387 cells. Knockdown of
379 *ALKBH5* resulted in decreased cell proliferation and impaired invasion and migration
380 capabilities, further confirming the critical role of *ALKBH5* in regulating the malignancy of
381 HCC cells. Corroborating previous studies, *ALKBH5*, recognized as a prominent m6A
382 demethylase(23), has been identified as a key player in a diverse array of cancers, such as breast
383 carcinoma, stomach carcinoma, and colorectal carcinoma(24, 25). The versatile roles of
384 *ALKBH5* in various cancer types entail the modulation of numerous biological processes
385 encompassing proliferation, metastasis, migration, invasion, metastasis, as well as tumor
386 growth. Interestingly, the influence of *ALKBH5* appears to be context-dependent, with its
387 expression level acting either as an oncogenic promoter or a tumor suppressor, depending on
388 the type of carcinoma(26, 27). Further supporting its multifaceted role, recent evidence also
389 points towards an intriguing interaction between *ALKBH5* and *NEAT1* in colorectal carcinoma,
390 proposing the ALKBH5-NEAT1 axis as a potential therapeutic target(28). Taken together, our
391 findings underscore *ALKBH5* as an influential factor in the pathogenesis of HCC. More
392 thorough and in-depth research are needed, however, to elucidate the specific processes by
393 which *ALKBH5* promotes HCC development and to prove its efficacy in clinical settings.
394 In the subsequent phase of our study, we performed a differential gene expression screen on
395 HCC patients, based on *ALKBH5* expression levels. In the KEGG pathway analysis, the up-
396 regulated DEGs-enriched KEGG pathways include Wnt signaling pathway, Renal cell
397 carcinoma, and the Hippo signaling pathway. Shuai He et al. postulated that the WNT/β-catenin
398 signaling pathway, a highly conserved and tightly controlled molecular mechanism, governs
399 cellular differentiation, proliferation, and embryonic development(29). Notably, there is

increasing evidence that abnormalities in WNT/β-catenin signaling contribute to the progression and development of liver carcinoma, which contained HCC and cholangiocarcinoma(30, 31). In addition, when Takebumi Usui et al. studied cases of renal cell carcinoma liver metastases, they found that many patients with renal cell carcinoma after surgical resection would develop in the direction of liver carcinoma(32). The Hippo pathway was found to be a critical regulator of liver size, metabolism, development, regeneration, and homeostasis in genetic studies on murine livers conducted by Jordan H. Driskill and Duojia Pan. Abnormalities in this pathway may contribute to common liver diseases like liver carcinoma and fatty liver disease(33). Besides, the down-regulated DEGs are abundant in Tryptophan metabolism, Retinol metabolism, Pyruvate metabolism, Histidine and Glutathione metabolism. This underlines the intricate interplay between liver carcinoma and functional molecular metabolism within the human body. For instance, research by Qunhua Han et al. delineates an age-related metabolic imbalance in the liver involving glycerophospholipids, arachidonic acid, histidine, and linoleic acid(34). In summary, our exploration of the roles of various metabolic and signaling pathways provides valuable insights into the molecular landscape of HCC, highlighting the potential for targeting these specific pathways for therapeutic intervention.

Through PFS survival, PPI, correlation, LASSO, Cox and other prognostic value analyses, we identified 6 key genes (*HGFAC*, *SPP2*, *CFHR3*, *ADNP*, *ACIN1*, *TTI1*) associated with HCC prognosis. Following that, we used the GEPIA database to determine the connection between *ALKBH5* and these genes, finally identifying *TTI1* as the most significant prognostic gene.

TTI1, or TELO2 Interacting Protein 1, plays a vital role in various biological processes, yet remains relatively understudied. Existing literature suggests that *TTI1* is involved in multiple metabolic pathways and in the activation of mTORC1 signaling, which promotes cell growth(35, 36). For instance, *TTI1* has been shown to facilitate survival in multiple myeloma via the mTORC1 pathway(37). Rao et al. revealed the role of *TTI1* in binding ATM and DNA-PKcs, triggering the activation of p-53 and S-15 phosphorylation pathways to initiate cancer cell death programs(38). Furthermore, research on colorectal cancer by Peng Xu et al. indicated higher *TTI1* expression in tumor tissue relative to adjacent normal tissue, demonstrating its critical role in colorectal cancer proliferation(39). Nevertheless, the influence of *TTI1* on the development of liver carcinoma is still not clear.

We conducted a thorough study to investigate the function of *TTI1* in HCC, and the findings underscored the importance of both *TTI1* and *ALKBH5* in the development of HCC. TTI1 was discovered to be considerably overexpressed in HCC tumors as compared to normal tissues. Notably, *ALKBH5* overexpression was seen to significantly enhance SNU387 cell proliferation, an effect inversely mirrored by *TTI1* under-expression. *TTI1* also emerged as an independent prognostic indicator for overall survival in HCC patients, prompting us to construct a predictive *TTI1* nomogram with high consistency between predicted and actual survival rates. The interaction between *TTI1* and *ALKBH5* revealed their influence on HCC cell growth. Downregulation of *TTI1* suppressed cell proliferation, migration and invasion, a result that was partially counteracted by *ALKBH5* overexpression. *TTI1* overexpression, on the other hand, enhanced cell proliferation, migration, and invasion but was inhibited by reduced *ALKBH5*

expression. Altogether, these findings underscore a potential regulatory role of *ALKBH5* in HCC progression via modulation of *TTI1* expression, illuminating novel avenues for potential therapeutic strategies.

To sum up, our findings confirm the characterization of *ALKBH5* and *TTI1* as oncogenes in HCC, emphasizing their potential as novel markers in HCC. Through bioinformatics analysis and cellular experiments, we elucidated that the interaction between ALKBH5 and TTI1 significantly affects the proliferation, migration and invasion of HCC cells, suggesting that ALKBH5 may exert a key regulatory influence on HCC progression by regulating TTI1 expression. These findings greatly advance the current understanding of HCC and pave the way for innovative directions for future research.

Author Contributions

Conception and design of the research: Zhiqiu Hu and Ziping Zhang.

Acquisition of data: Xubo Wu and Jinfeng Feng and Huarong Mao.

Analysis and interpretation of data: Xiang Zhou and Qimeng Chang.

Statistical analysis: Qimeng Chang and Zhiqiu Hu.

Drafting the manuscript: Zhiqiu Hu and Xiang Zhou.

Revision of manuscript for important intellectual content: Ziping Zhang and Qimeng Chang.

465 **REFERENCE**

466 1. Hatta MNA, Mohamad Hanif EA, Chin SF, Neoh HM. Pathogens and Carcinogenesis: A
467 Review. Biology (Basel). 2021;10(6).

468 2. Kiani A, Uyumazturk B, Rajpurkar P, Wang A, Gao R, Jones E, et al. Impact of a deep
469 learning assistant on the histopathologic classification of liver cancer. NPJ Digit Med.
470 2020;3:23.

471 3. Montella M, Crispo A, Giudice A. HCC, diet and metabolic factors: Diet and HCC. Hepat
472 Mon. 2011;11(3):159-62.

473 4. Hwang S, Lee SG, Belghiti J. Liver transplantation for HCC: its role: Eastern and Western
474 perspectives. J Hepatobiliary Pancreat Sci. 2010;17(4):443-8.

475 5. Bruix J, Sherman M, Practice Guidelines Committee AAftSoLD. Management of
476 hepatocellular carcinoma. Hepatology. 2005;42(5):1208-36.

477 6. Reig M, da Fonseca LG, Faivre S. New trials and results in systemic treatment of HCC. J
478 Hepatol. 2018;69(2):525-33.

479 7. Page AJ, Cosgrove DC, Philosophe B, Pawlik TM. Hepatocellular carcinoma: diagnosis,
480 management, and prognosis. Surg Oncol Clin N Am. 2014;23(2):289-311.

481 8. Wang J, Wang J, Gu Q, Ma Y, Yang Y, Zhu J, et al. The biological function of m6A
482 demethylase ALKBH5 and its role in human disease. Cancer Cell Int. 2020;20:347.

483 9. Guo X, Li K, Jiang W, Hu Y, Xiao W, Huang Y, et al. RNA demethylase ALKBH5 prevents
484 pancreatic cancer progression by posttranscriptional activation of PER1 in an m6A-YTHDF2-
485 dependent manner. Mol Cancer. 2020;19(1):91.

486 10. Yang Q, Liang Y, Shi Y, Shang J, Huang X. The ALKBH5/SOX4 axis promotes liver

487 cancer stem cell properties via activating the SHH signaling pathway. Journal of Cancer
488 Research and Clinical Oncology. 2023;149(17):15499-510.
489 11. Liu H, Jiang Y, Lu J, Peng C, Ling Z, Chen Y, et al. m6A-modification regulated circ-
490 CCT3 acts as the sponge of miR-378a-3p to promote hepatocellular carcinoma progression.
491 Epigenetics. 2023;18(1):2204772.
492 12. Chen Y, Zhou P, Deng Y, Cai X, Sun M, Sun Y, et al. ALKBH5-mediated m6 A
493 demethylation of TIRAP mRNA promotes radiation-induced liver fibrosis and decreases
494 radiosensitivity of hepatocellular carcinoma. Clin Transl Med. 2023;13(2):e1198.
495 13. Zhang H, Liu Y, Wang W, Liu F, Wang W, Su C, et al. ALKBH5-mediated m6A
496 modification of lincRNA LINC02551 enhances the stability of DDX24 to promote
497 hepatocellular carcinoma growth and metastasis. Cell Death & Disease. 2022;13(11):926.
498 14. You Y, Wen D, Zeng L, Lu J, Xiao X, Chen Y, et al. ALKBH5/MAP3K8 axis regulates
499 PD-L1+ macrophage infiltration and promotes hepatocellular carcinoma progression.
500 International Journal of Biological Sciences. 2022;18(13):5001-18.
501 15. Shen C, Sheng Y, Zhu AC, Robinson S, Chen J. RNA Demethylase ALKBH5 Selectively
502 Promotes Tumorigenesis and Cancer Stem Cell Self-Renewal in Acute Myeloid Leukemia. Cell
503 Stem Cell. 2020;27(1).
504 16. Shen C, Sheng Y, Zhu AC, Robinson S, Jiang X, Dong L, et al. RNA Demethylase
505 ALKBH5 Selectively Promotes Tumorigenesis and Cancer Stem Cell Self-Renewal in Acute
506 Myeloid Leukemia. Cell Stem Cell. 2020;27(1):64-80 e9.
507 17. Akanda MR, Park JS, Noh MG, Ha GH, Park YS, Lee JH, et al. TACC3 Promotes Gastric
508 Carcinogenesis by Promoting Epithelial-mesenchymal Transition Through the ERK/Akt/cyclin

509 D1 Signaling Pathway. Anticancer Res. 2021;41(7):3349-61.

510 18. Carneiro BA, Elvin JA, Kamath SD, Ali SM, Paintal AS, Restrepo A, et al. FGFR3-TACC3:
511 A novel gene fusion in cervical cancer. Gynecol Oncol Rep. 2015;13:53-6.

512 19. Fan X, Liu B, Wang Z, He D. TACC3 is a prognostic biomarker for kidney renal clear cell
513 carcinoma and correlates with immune cell infiltration and T cell exhaustion. Aging (Albany
514 NY). 2021;13(6):8541-62.

515 20. Ha GH, Park JS, Breuer EK. TACC3 promotes epithelial-mesenchymal transition (EMT)
516 through the activation of PI3K/Akt and ERK signaling pathways. Cancer Lett. 2013;332(1):63-
517 73.

518 21. Toh MR, Wong EYT, Wong SH, Ng AWT, Loo L-H, Chow PK-H, et al. Global
519 epidemiology and genetics of hepatocellular carcinoma. Gastroenterology. 2023;164(5):766-
520 82.

521 22. Valenti L, Pedica F, Colombo M. Distinctive features of hepatocellular carcinoma in non-
522 alcoholic fatty liver disease. Digestive and Liver Disease. 2022;54(2):154-63.

523 23. Wang J, Wang J, Gu Q, Ma Y, Yang Y, Zhu J, et al. The biological function of m6A
524 demethylase ALKBH5 and its role in human disease. Cancer cell international. 2020;20(1):1-
525 7.

526 24. Guo T, Liu D-F, Peng S-H, Xu A-M. ALKBH5 promotes colon cancer progression by
527 decreasing methylation of the lncRNA NEAT1. American Journal of Translational Research.
528 2020;12(8):4542.

529 25. Qu J, Yan H, Hou Y, Cao W, Liu Y, Zhang E, et al. RNA demethylase ALKBH5 in cancer:
530 from mechanisms to therapeutic potential. Journal of hematology & oncology. 2022;15(1):1-

24.

26. Dong S, Wu Y, Liu Y, Weng H, Huang H. N6-methyladenosine Steers RNA Metabolism and Regulation in Cancer. Cancer Communications. 2021;41(7):538-59.

27. Xue J, Xiao P, Yu X, Zhang X. A positive feedback loop between AlkB homolog 5 and miR-193a-3p promotes growth and metastasis in esophageal squamous cell carcinoma. Human Cell. 2021;34(2):502-14.

28. Guo T, Liu DF, Peng SH, Xu AM. ALKBH5 promotes colon cancer progression by decreasing methylation of the lncRNA NEAT1. Am J Transl Res. 2020;12(8):4542-9.

29. He S, Tang S. WNT/beta-catenin signaling in the development of liver cancers. Biomed Pharmacother. 2020;132:110851.

30. Wei S, Dai M, Zhang C, Teng K, Wang F, Li H, et al. KIF2C: a novel link between Wnt/β-catenin and mTORC1 signaling in the pathogenesis of hepatocellular carcinoma. Protein & Cell. 2021;12(10):788-809.

31. He S, Tang S. WNT/β-catenin signaling in the development of liver cancers. Biomedicine & Pharmacotherapy. 2020;132:110851.

32. Usui T, Kuhara K, Nakayasu Y, Tsuchiya A, Shimojima Y, Kono T, et al. [Four Cases of Liver Resection for Liver Metastases from Renal Cell Carcinoma]. Gan To Kagaku Ryoho. 2021;48(13):1700-2.

33. Driskill JH, Pan D. The Hippo Pathway in Liver Homeostasis and Pathophysiology. Annu Rev Pathol. 2021;16:299-322.

34. Han Q, Li H, Jia M, Wang L, Zhao Y, Zhang M, et al. Age-related changes in metabolites in young donor livers and old recipient sera after liver transplantation from young to old rats.

553 Aging Cell. 2021;20(7):e13425.

554 35. Zhang LX, Yang X, Wu ZB, Liao ZM, Wang DG, Chen SW, et al. TTI1 promotes non-
555 small-cell lung cancer progression by regulating the mTOR signaling pathway. Cancer Science.
556 2023;114(3):855.

557 36. Bakan I, Laplante M. Connecting mTORC1 signaling to SREBP-1 activation. Current
558 opinion in lipidology. 2012;23(3):226-34.

559 37. Li J, Zhu J, Cao B, Mao X. The mTOR signaling pathway is an emerging therapeutic target
560 in multiple myeloma. Curr Pharm Des. 2014;20(1):125-35.

561 38. Rao F, Cha J, Xu J, Xu R, Vandiver MS, Tyagi R, et al. Inositol Pyrophosphates Mediate
562 the DNA-PK/ATM-p53 Cell Death Pathway by Regulating CK2 Phosphorylation of Tti1/Tel2.
563 Mol Cell. 2020;79(4):702.

564 39. Xu P, Du G, Guan H, Xiao W, Sun L, Yang H. A role of TTI1 in the colorectal cancer by
565 promoting proliferation. Transl Cancer Res. 2021;10(3):1378-88.

566

567

TABLES AND FIGURES WITH LEGENDS

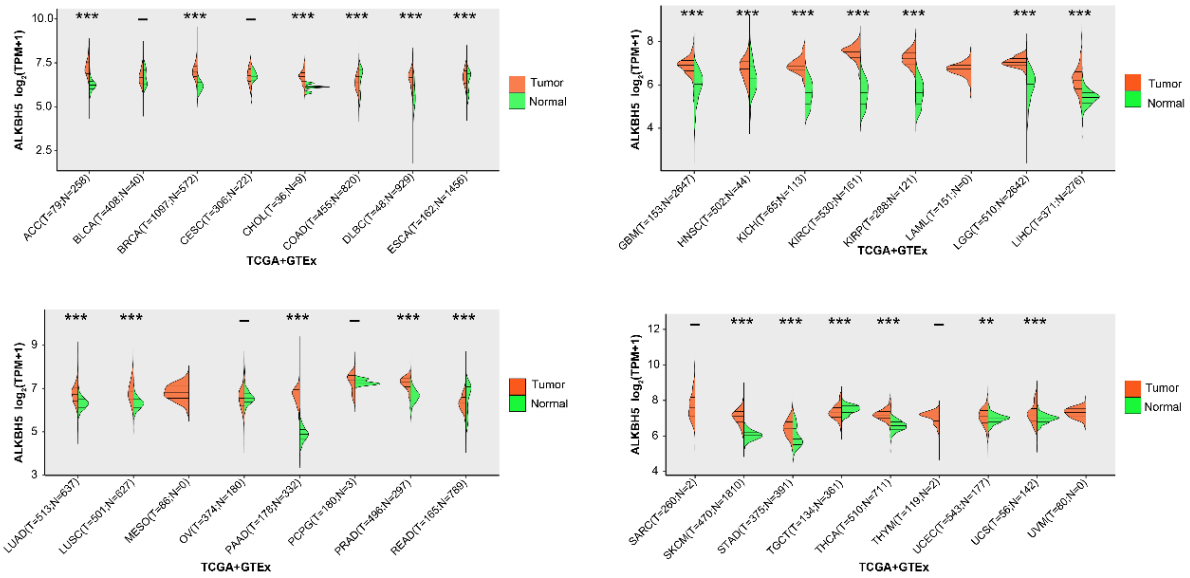

Figure 1. **Expression verification of *ALKBH5* in 33 tumors.** The abscissa represents the tumor and normal samples in the TCGA and GTEx databases, the ordinate represents the expression distribution of ALKBH5, and different colors represent different groups. $^{**}P < 0.01$, $^{***}P < 0.001$. TCGA: The Cancer Genome Atlas; GTEx: Genotype-Tissue Expression.

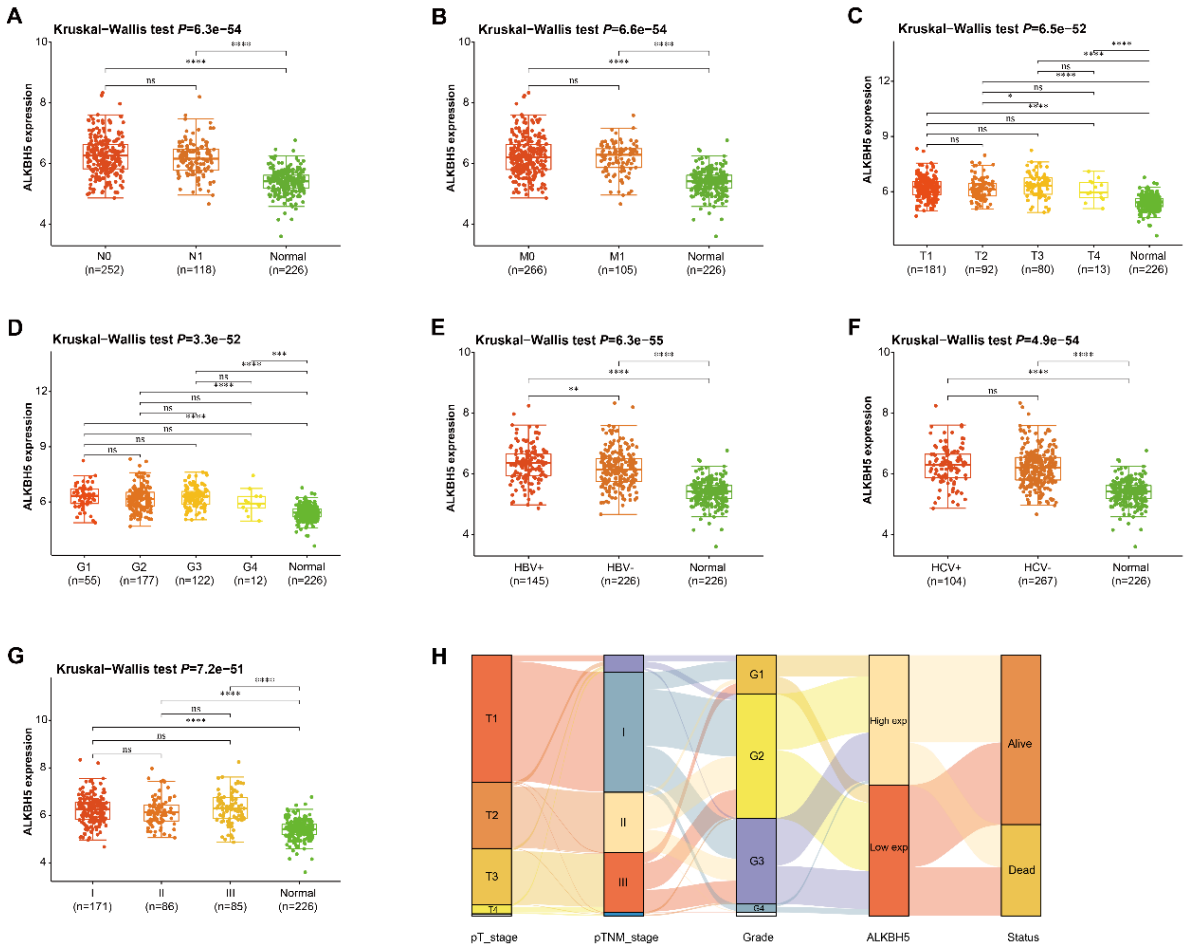

Figure 2. ALKBH5 expressions in HCC patients with different clinical factors. (A-G) Kruskal-Wallis test ALKBH5 expression in lymph node metastasis status, distant metastasis, pT stage, Gage, hepatitis B virus infection, hepatitis C virus infection and pTNM stage. $^{**}P < 0.01$, $^{***}P < 0.001$, $^{****}P < 0.0001$, ns means not statistically significant. (H) Sankey diagram. Every column stands for a characteristic variable, different colors stand for different types or stages, and the lines stand for the distribution of the same sample in different characteristic variables. HCC: Hepatocellular carcinoma; pTNM: Pathological tumor, node, metastasis.

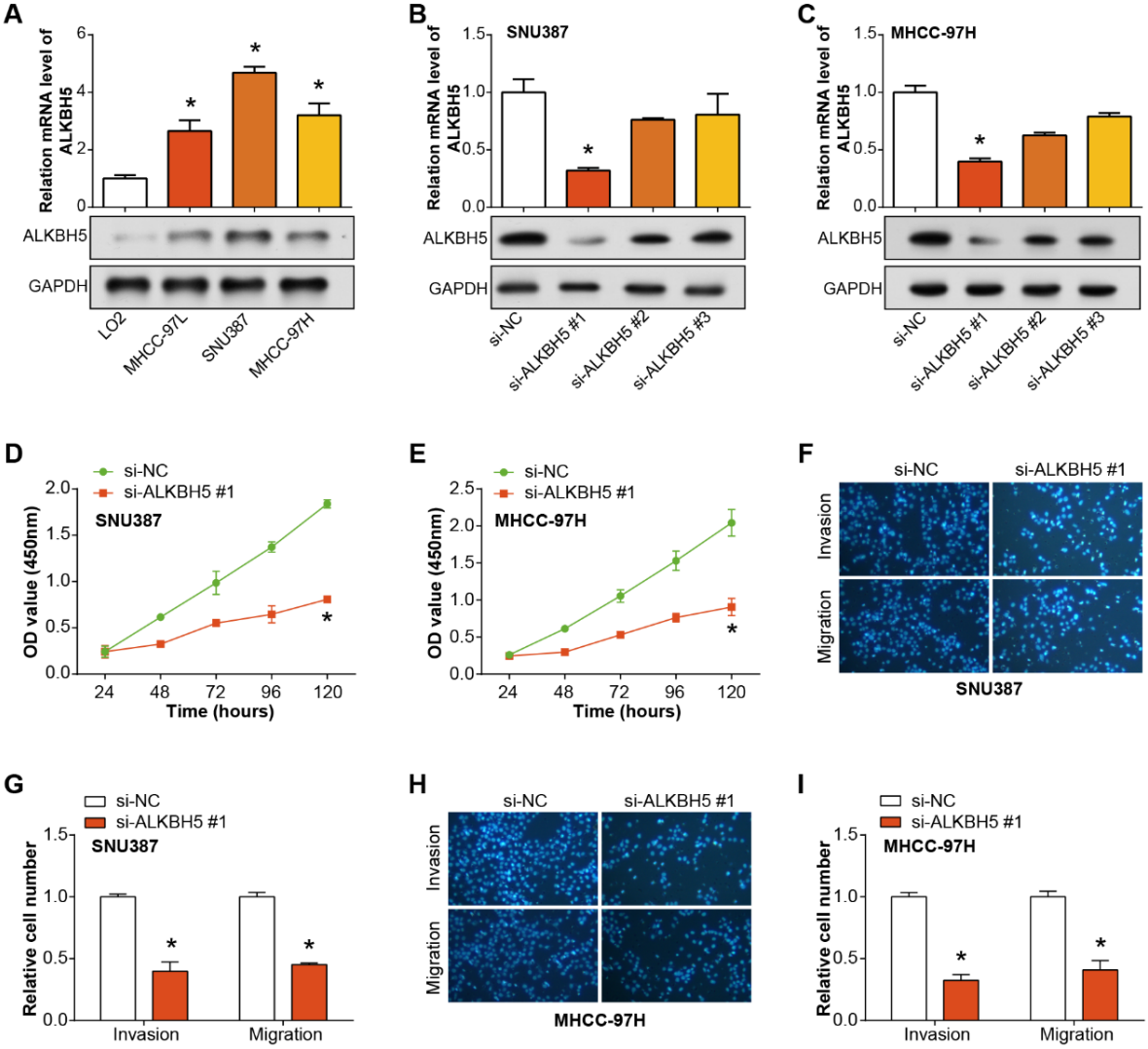

Figure 3. Expression and functional analysis of ALKBH5 in normal and HCC cell lines. (A) qRT-PCR and WB detection of ALKBH5 expression levels in normal cells and HCC cell lines. (B) qRT-PCR and WB detection of knockdown efficiency of ALKBH5 in SNU387 cells. (C) qRT-PCR and WB detection of knockdown efficiency of ALKBH5 in MHCC-97H cells. (D and E) CCK-8 detects the regulation of si-ALKBH5#1 on the proliferation of SNU387 and MHCC-97H cells. (F-I) Transwell detection of the regulation of si-ALKBH5#1 on the invasion and migration of SNU387 and MHCC-97H cells. The left panel shows magnified field views, while the right panel represents the quantified bar graphs. *$P < 0.05$. HCC: Hepatocellular carcinoma; WB: Western blot; CCK-8: Cell counting kit-8.

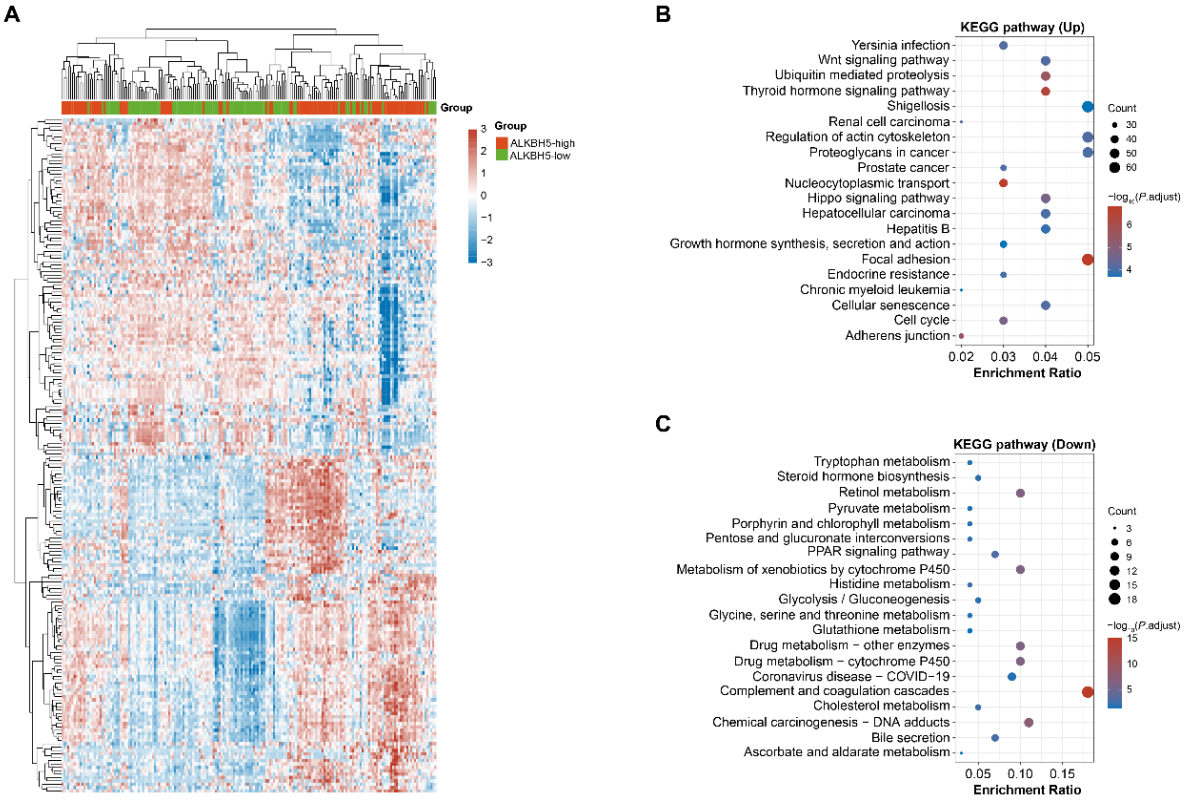

Figure 4. Distribution and pathway enrichment analysis of DEGs in HCC samples based on ALKBH5 expression levels. (A) Heat map of cluster distribution of up-regulated DEGs and down-regulated DEGs in HCC samples with high and low expression of ALKBH5. (B and C) Bubble plots of KEGG pathway enrichment analysis for up-regulated and down-regulated DEGs. Each bubble in the plot represents a different KEGG pathway, the size of the bubble corresponds to the number of DEGs associated with a particular pathway, and the color of the bubble represents the significance of the enrichment. DEG: Differentially expressed genes; HCC: Hepatocellular carcinoma; KEGG: Kyoto Encyclopedia of Genes and Genomes.

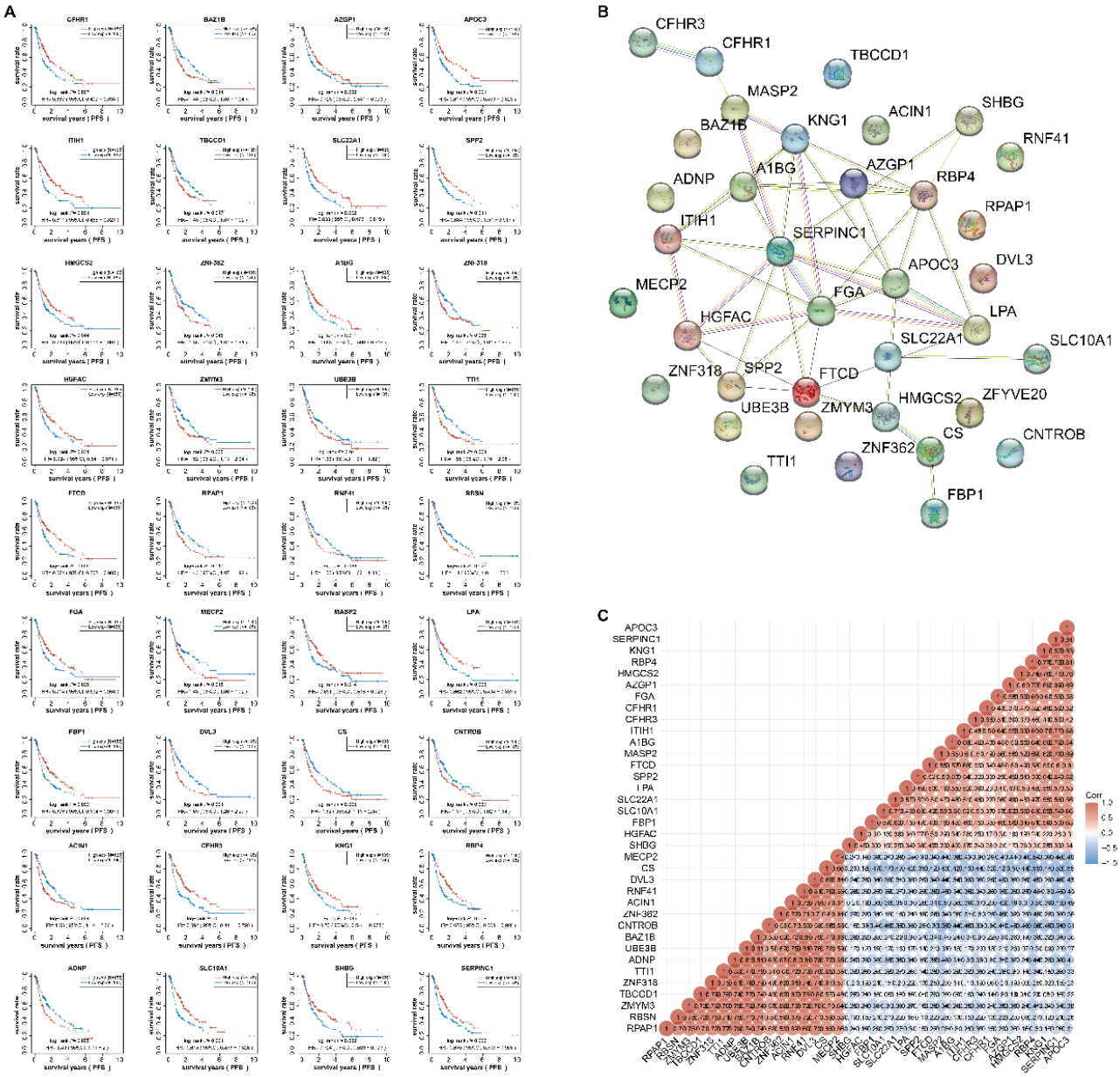

Figure 5. Bioinformatics analysis of 36 genes with significant prognostic value in HCC. (A) KM survival curves for 36 genes with significant *P* values, the horizontal axis represents the survival time, and the vertical axis represents the survival probability. (B) PPI network of 36 genes, nodes represent genes and edges represent interconnections between genes. (C) Correlation heat map of 36 genes, the abscissa and ordinate represent genes, red represents positive correlation, blue represents negative correlation. HCC: Hepatocellular carcinoma; KM: Kaplan-Meier; PPI: Protein-protein interactions.

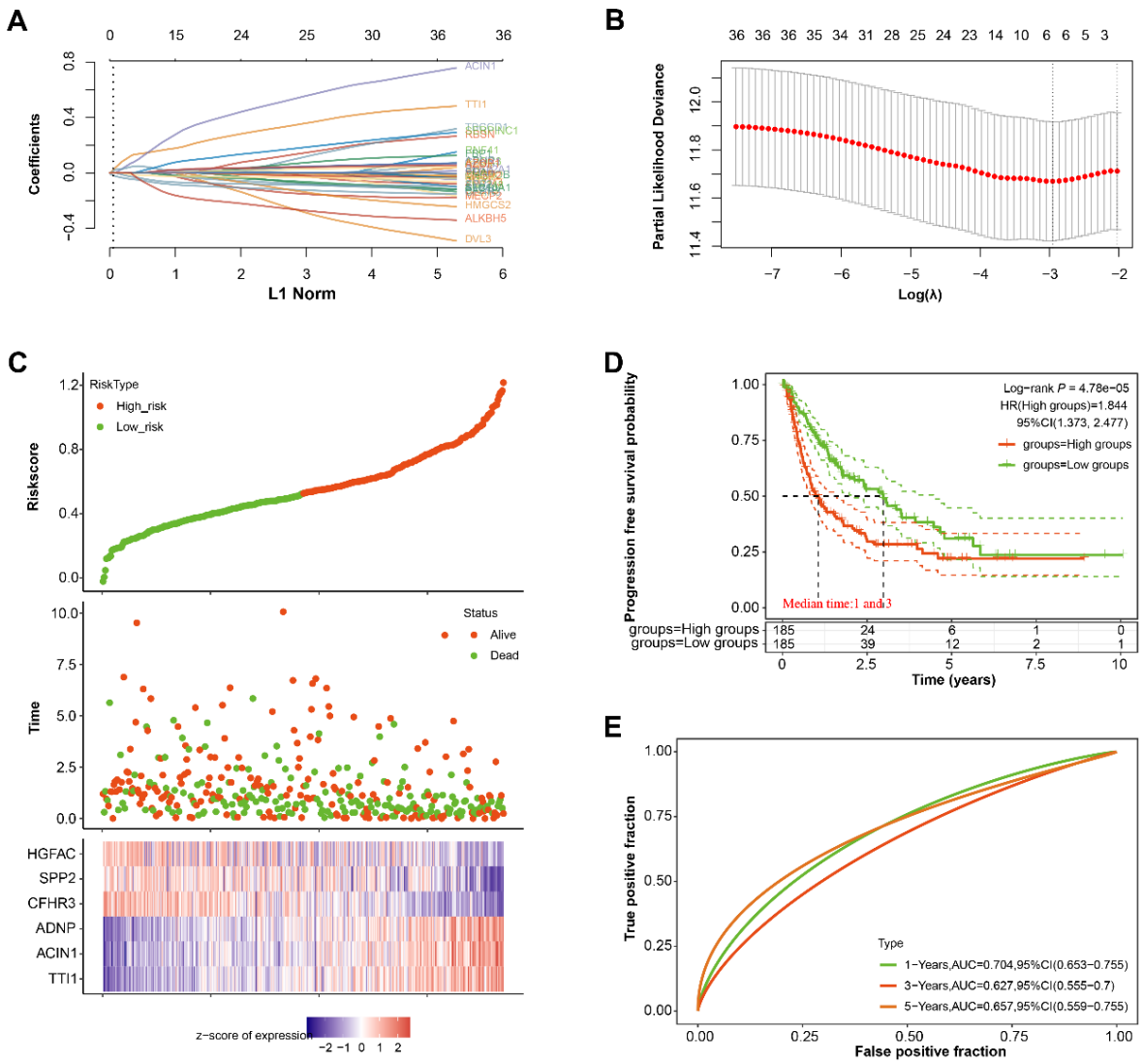

Figure 6. The identification of key gene with prognostic value related to ALKBH5 and HCC. (A) LASSO coefficient profile of 36 genes, different colored lines represent different genes. (B) LASSO regression with ten-fold cross-validation obtained 6 prognostic genes using the minimum λ value. (C) The upper panel shows the risk score distribution of HCC patients, the middle panel represents the survival status of patients, and the lower panel is a heatmap of the expression profiles of the six prognostic genes. (D) KM survival curves showing the difference in PFS between high-risk and low-risk samples, with a median time of 1 and 3 years for the two groups of samples. (E) ROC analysis of the risk model, curves showing the true positive rate (sensitivity) versus the false positive rate (1-specificity) for different cut-off points of the risk score. LASSO: Least Absolute Shrinkage and Selection Operator; HCC: Hepatocellular carcinoma; KM: Kaplan-Meier; PFS: Progression-free survival; ROC: Receiver operating characteristic.

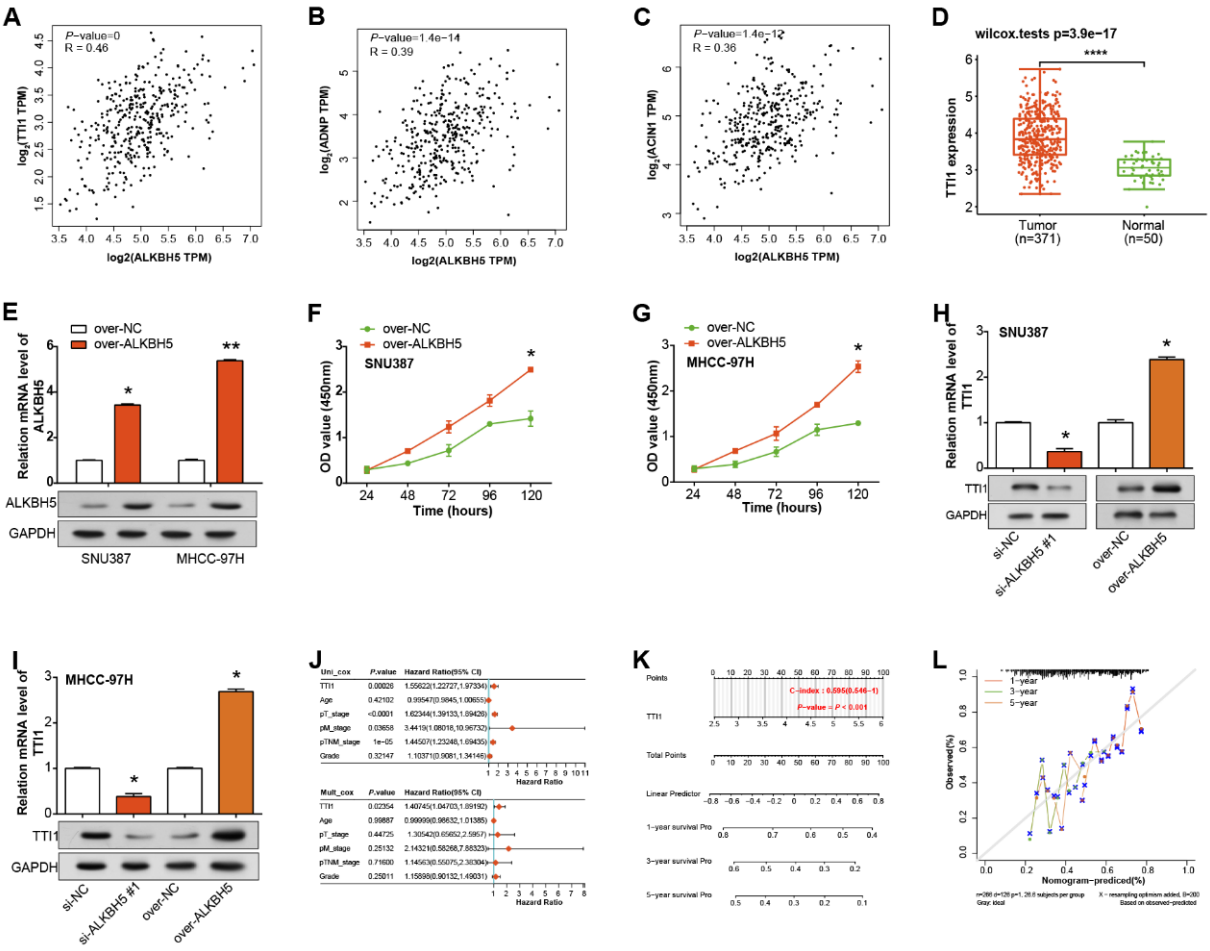

Figure 7. The construction of predicative nomogram for HCC prognosis. (A-C) Scatterplots of correlation analysis of ALKBH5 with TTI1, ADNP, and ACIN1 in the GEPIA database. Statistically significant *P*-values and correlation coefficient r values are shown in the upper left corner of each graph. (D) Boxplot of TTI1 expression levels in normal samples and HCC samples. (E) qRT-PCR and WB detection of overexpression efficiency of ALKBH5 in SNU387 as well as MHCC-97H cells. (F and G) Regulation of over-ALKBH5 on the proliferation of SNU387 and MHCC-97H cells in CCK-8 assay. (H and I) qRT-PCR and WB detected the regulation of TTI1 expression level by knockdown or overexpression of ALKBH5 in SNU387 cells. (J) Univariate and multivariate Cox analysis of TTI1 and clinical characteristics (pT stage, pM stage, pTNM stage, Grade). (K) Nomogram predicting the effect of TTI1 on the 1-, 3-, and 5-year survival of HCC patients. (L) Calibration curve of the overall survival nomogram model in TTI1, the diagonal dashed line stands for the ideal nomogram and the red, yellow and grey lines stand for the observed 1-, 3- and 5-year prognosis. *$P<0.05$, **$P<0.01$, ****$P<0.0001$. HCC: Hepatocellular carcinoma; pTNM: Pathological tumor, node, metastasis; CCK-8: Cell counting kit-8.

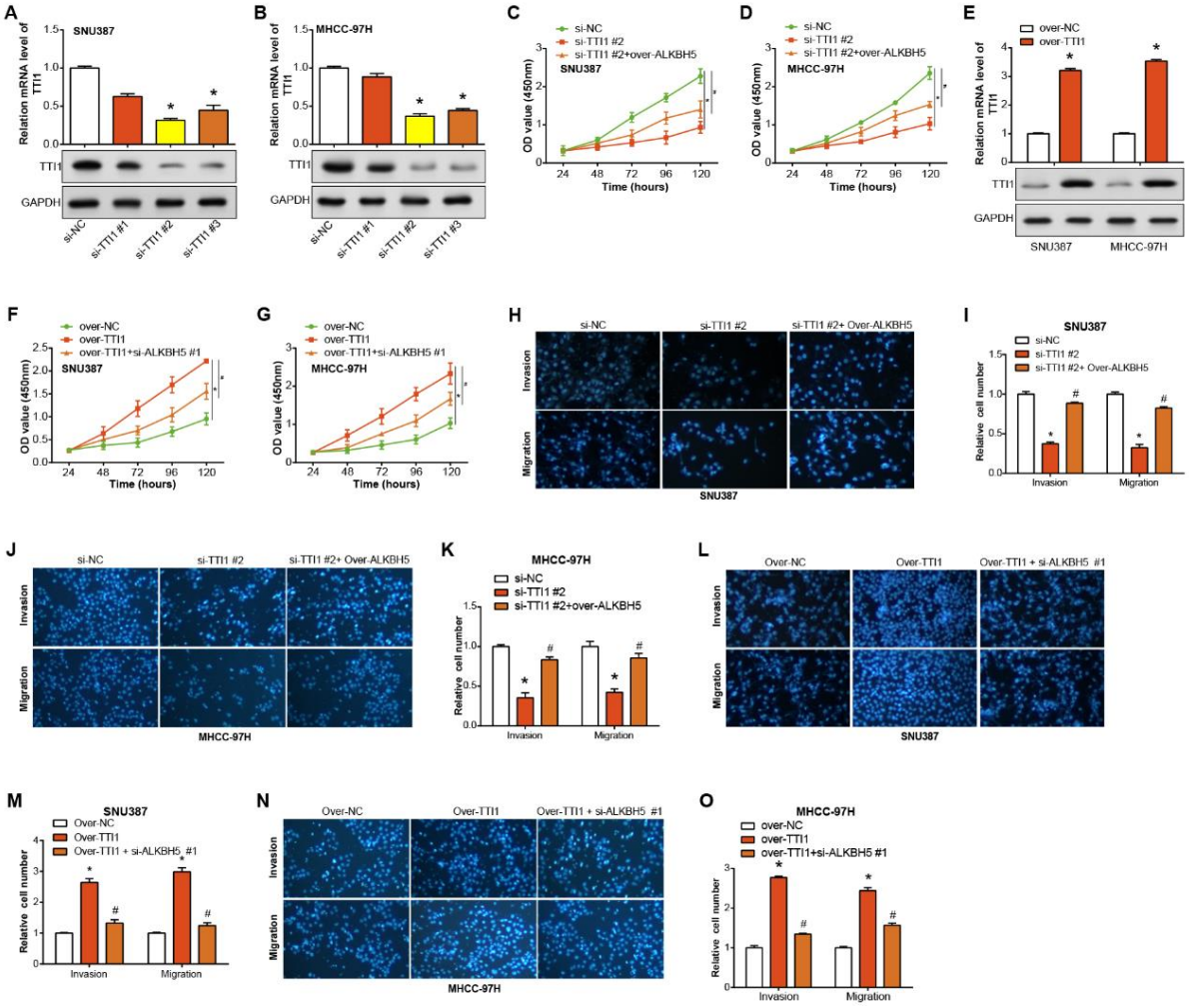

Figure 8. Influence of TTI1 and ALKBH5 on cell proliferation, migration, and invasion in HCC cells. (A and B) The relative expression of *TTI1* mRNA in SNU387 and MHCC-97H cells transfected with si-TTI1#1, #2 and #3 was detected by qRT-PCR. (C and D) CCK-8 test for the regulation of cell proliferation by si-TTI1#2 combined with over-ALKBH5. (E) qRT-PCR detection of the overexpression efficiency of TTI1 in SNU387 and MHCC-97H cells. (F and G) CCK-8 test for the regulation of over-TTI1 combined with si-ALKBH5#1 on cell proliferation. (H-K) Transwell assay analysis of the regulation of si-TTI1#2 and over-ALKBH5 on cell migration and invasion. (L-O) Transwell assay analysis of the regulation of over-TTI1 combined with si-ALKBH5#1 on cell proliferation. *P<0.05 vs. si-NC or over-NC, #P<0.05 vs si-TTI1 #2 or over-TTI1. HCC: Hepatocellular carcinoma; CCK-8: Cell counting kit-8; NC: Normal control.